

A device for studies of the early stages of post-spinning crystallization in polymer fibres

H. A. Hristov and J. M. Schultz

Materials Science Program, University of Delaware, Newark, DE 19716, USA

(Received 12 October 1987; accepted 18 November 1987)

An apparatus for investigation of the early stages of crystallization under tension of polymeric fibres has been constructed. The heating time of poly(ethylene terephthalate) fibre with filament diameter of $20\ \mu\text{m}$ was measured to be about 16 ms at a heating rate of $10^4\ \text{K s}^{-1}$. The experimental results showed multistage crystallization at low stress. At high stress and temperatures, the crystallization process exhibits only one stage. The activation energy of the process and the crystallization velocity are derived.

(Keywords: crystallization; fibres; poly(ethylene terephthalate))

INTRODUCTION

The study of post-spinning crystallization of polymer fibres is important for two reasons. One reason is the commercial importance of such processing—found in most commercial fibre spinning, with the exception of some ultra-high-speed lines. The second reason is that such crystallization is prototypical of crystallization under high chain orientation, a process that appears to be qualitatively different from quiescent crystallization and about whose details and kinetics startlingly little is known.

A number of studies of post-spinning crystallization kinetics in poly(ethylene terephthalate) (PET)¹⁻¹⁰ and nylon^{11,12} have been reported. In general, the overall rate of crystallization increases remarkably with threadline stress and with temperature. At moderate stresses and temperatures, crystallization half-times are typically tens of milliseconds. In that time regime, a multistage process appears to occur^{7,9,12}. But the experiments needed to study the separate time regimes have not been performed, largely because heat transfer to the fibre has been too slow to reach a quasi-isothermal state quickly enough. Further, behaviour at higher stresses and temperatures has also not been studied, because extant systems do not possess the low heat transfer time and high data collection speed necessary to probe the earliest phases of transformation.

Described here is an instrument designed specifically to probe the early kinetics ($< 300\ \text{ms}$) of transformations in fibres. Described also are preliminary results showing multistage kinetics.

EXPERIMENTAL

The investigations were carried out on poly(ethylene terephthalate) (PET) fibres from the Rhône-Poulenc Company, melt-spun at $3300\ \text{m min}^{-1}$ and subsequently quenched. Each fibre was a bundle of ~ 30 filaments with a filament diameter of $20\ \mu\text{m}$.

In order to achieve a very rapid heating rate, to reach

an isothermal regime in some hundredths of a second, and in order to make *in situ* measurements of the changes in the length of the fibre at precisely determined tension, an apparatus based on the principle of 'splash heating' was constructed. In Figure 1 are shown schematically the basic components of this device.

A low-melting metal alloy is heated in the copper vessel (A). A GaInSn alloy, with $T_m = 40^\circ\text{C}$ was used. The bottom of A is made with holes ($d = 1\ \text{mm}$). Capillary force holds the liquid metal in the vessel at temperatures higher than T_m . When the desired temperature is reached, the electromagnetic valve (V) opens and gas under pressure (argon at 2.5 atm) rapidly fills the volume of A. In this way, the liquid alloy is 'splashed' in the Teflon vessel (B) and heats the fibre, which is stretched on a copper strip on the bottom of B. The changes of the length of the sample are transferred to the core of a linear variable differential transformer (LVDT) by a system of ball-bearings. The signal from the LVDT is digitized and conditioned (Keithley DAS500) and the data fed into a personal computer (IBM PC/AT) for storage and further processing. The sampling time used for the present experiments was 3.5 ms. The fibre tension was set by the weight (M).

The time required to bring a fibre to the treatment

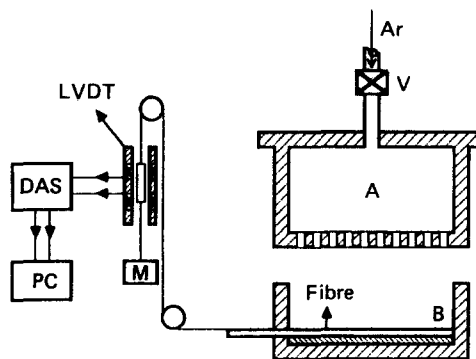


Figure 1 Fibre heat-treatment apparatus (see text for details)

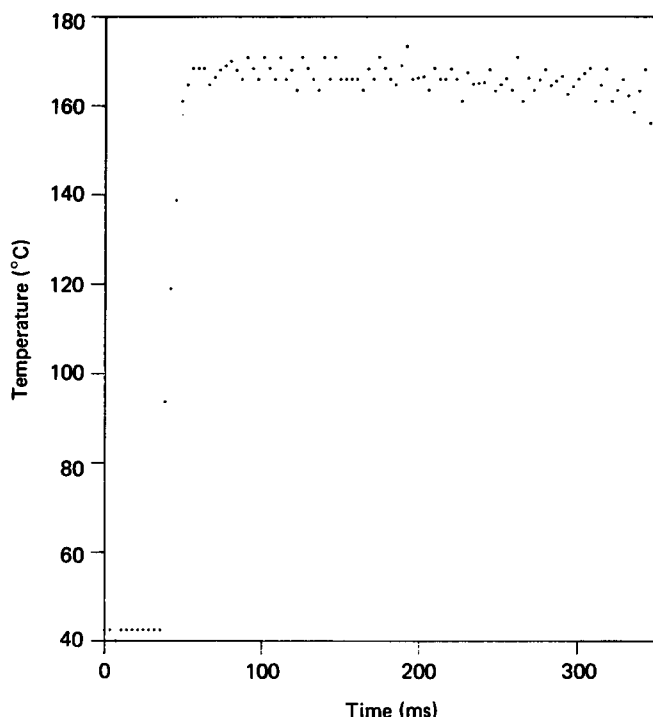


Figure 2 Time-temperature curve for copper-constantan thermocouple (with displaced zeros)

temperature was determined by several independent methods:

(i) Using a copper-constantan thermocouple placed on the strip. Since the heating time depends on the coefficient of thermal diffusion of the material and on geometric factors, the diameter of the head of the thermocouple was chosen to correspond to the heating time of a PET filament with diameter of 20 μm .

(ii) By the thermal elongation of copper and stainless-steel wires with suitable diameters.

(iii) By the relaxation time of highly oriented semicrystalline PET fibre melt-spun at 6000 m min^{-1} .

(iv) By the thermal elongation of initially amorphous PET fibre, heated under stress several times in order to complete the crystallization.

All these experiments showed that the heating time* varies between 14 and 18 ms, corresponding to a heating rate of the order of 10^4 K s^{-1} .

As an example, on Figure 2 is shown the time-temperature curve for the copper-constantan thermocouple. It can be seen that the desired temperature is attained in some 16 ms. Thereafter, the temperature is effectively constant for 300 ms.

A heating time of 14–18 ms can also be directly derived from the initial elongation during the heat-treatment experiments. This will be demonstrated below, with reference to Figure 6.

The apparatus described above showed very good reproducibility of the results. For structural characterization of the as-spun polymer and the heat-treated samples, a Philips microcamera and Ni-filtered $\text{Cu K}\alpha$ radiation were used. A pinhole pattern of the as-spun fibres, shown in Figure 3a, is characterized by the absence of sharp diffraction spots or lines representative of a crystalline phase. The pattern is characterized also by a

clear orientation of the amorphous material along the fibre axis. The amorphous halo is more intense in the equatorial plane, evidence of chain orientation. More detailed diffractometric investigations revealed the presence of a small degree of crystallinity, estimated to be less than 1%. We can assume that the as-spun fibre is nearly amorphous, with moderate orientation of chains along the fibre axis (optical birefringence number 0.042) (ref. 9).

The isothermal kinetic investigations were carried out in the temperature range 140–230°C and with weights corresponding to threadline stresses (σ) of 72, 98 and 170 kg cm^{-2} .

Because of the fibre production method (quenching under tension), a relatively high internal stress is 'frozen' in the fibres. Data published for the same material⁹ show that during heat treatment under a stress of 21 kg cm^{-2} the fibres initially shrink at all temperatures, whereas shrinkage is observed only at lower temperatures under a stress of 53 kg cm^{-2} . This is an indication that the 'frozen' stress is between 50 and 60 kg cm^{-2} . For the present experiments, one can consider that after heating the 'net' internal stress—threadline stress minus frozen stress—is low (15–20 kg cm^{-2}), moderate (40–50 kg cm^{-2}) and high (110–120 kg cm^{-2}).

RESULTS

The results of the *in situ* measurements of the length change vs. time are summarized in Figures 4, 5 and 6, these three figures representing the three stress levels used. It can be seen that the process of elongation changes its character in the following way:

(a) At a low internal stress (Figure 4) and low temperature (140°C), the process is step-like with multiple steps. On increasing the temperature, three stages of elongation are observed, with decreasing induction time between them. For instance, the induction time between stages I and II is approximately 100 ms at 170°C, but is only 10 ms at 230°C.

(b) The third stage occurs after 300 ms, during the slow cooling of the fibre.

(c) Under moderate internal stress (Figure 5), the first two stages are merged into one and stage III is poorly expressed.

(d) Under high internal stress (Figure 6), the process has one stage, except at 140°C, where stage III can be seen. The first stage of transformation begins immediately, with no incubation time. The first approximately four data points above the baseline



Figure 3 (a) Pinhole pattern of as-spun PET fibre. (b) Pinhole pattern of PET fibre heat treated at $T = 140^\circ\text{C}$ and $\sigma = 72 \text{ kg cm}^{-2}$. (c) Pinhole pattern of PET fibre heat treated at $T = 230^\circ\text{C}$ and $\sigma = 170 \text{ kg cm}^{-2}$

* Heating time is the time taken to heat the sample to 90% of the desired treatment temperature

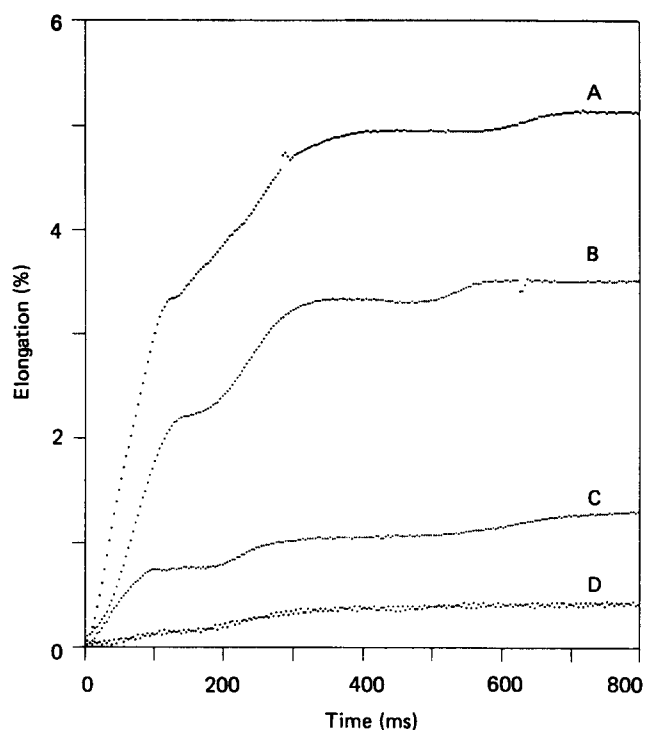


Figure 4 Elongation vs. time curves of PET fibres heat treated at $\sigma = 72 \text{ kg cm}^{-2}$ and (A) $T = 230^\circ\text{C}$, (B) 200°C , (C) 170°C and (D) 140°C

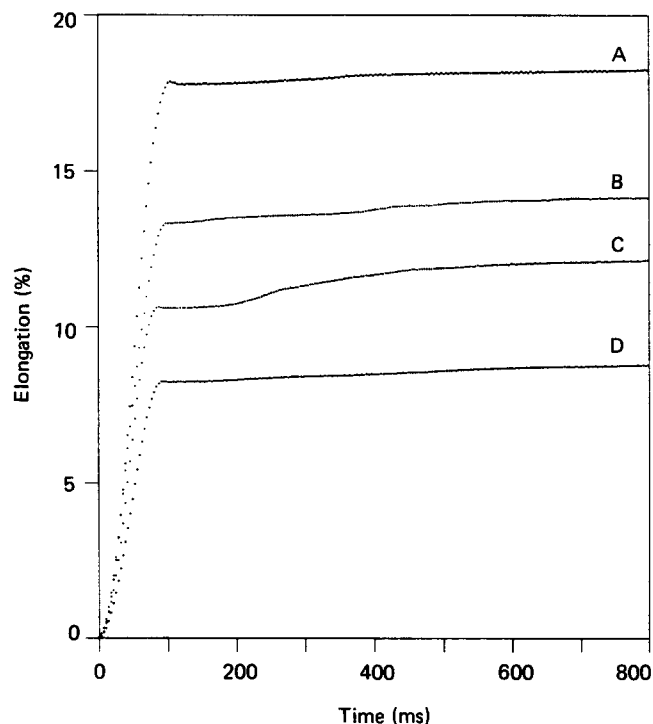


Figure 5 Elongation vs. time curves of PET fibres heat treated at $\sigma = 98 \text{ kg cm}^{-2}$ and (A) $T = 230^\circ\text{C}$, (B) 200°C , (C) 170°C and (D) 140°C

represent the heating of the fibre to the transformation temperature. When the normal thermal expansion associated with this heating is neglected, it is seen that the elongation begins with an initially high rate and proceeds approximately linearly with time.

From Figures 4, 5 and 6, it is clear that the final elongations (L_i) and the velocities of elongation (V_i) are affected by the external fields (temperature and stress). Higher stresses and temperatures lead to an increase of L_i

and to a well expressed linear character of the kinetics of the process. The V values under different conditions are determined from the linear portions of the curves. In the present experiments, the transformation temperature is approached from below. In such cases, the rate-controlling mechanism is generally the transport of matter, rather than interfacial attachments. One would expect such a process to follow a rate law with a simple activation energy expression. Under constant stress, the velocity is written as:

$$V(t) = V_0 \exp(-E_a/RT)$$

where V_0 is a constant, E_a is the activation energy and R is the gas constant.

Figure 7 shows that the variation of $V = f(T)$ can be presented as straight lines in plots of $\ln[V(T)]$ vs. $1/T$. (For $\sigma = 73 \text{ kg cm}^{-2}$ the velocities are derived from the slope of stage I.) The activation energies as determined

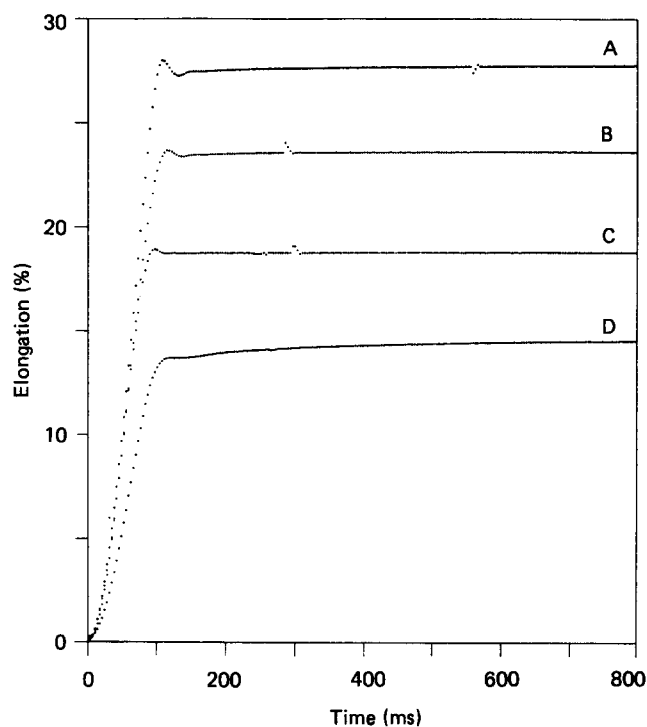


Figure 6 Elongation vs. time curves of PET fibres heat treated at $\sigma = 170 \text{ kg cm}^{-2}$ and (A) $T = 230^\circ\text{C}$, (B) 200°C , (C) 170°C and (D) 140°C

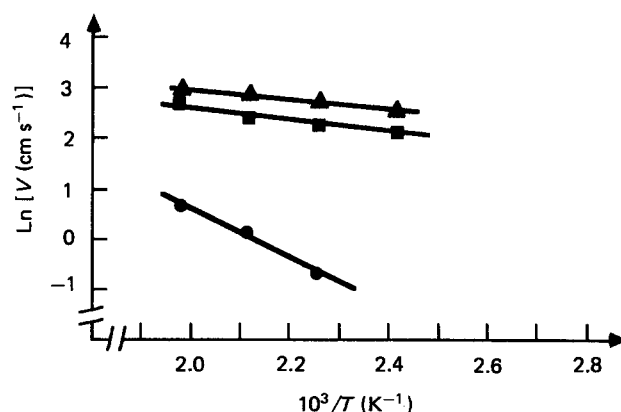


Figure 7 Velocity of elongation vs. inverse temperature for $\sigma = 72 \text{ kg cm}^{-2}$ (●), 98 kg cm^{-2} (■) and 180 kg cm^{-2} (▲)

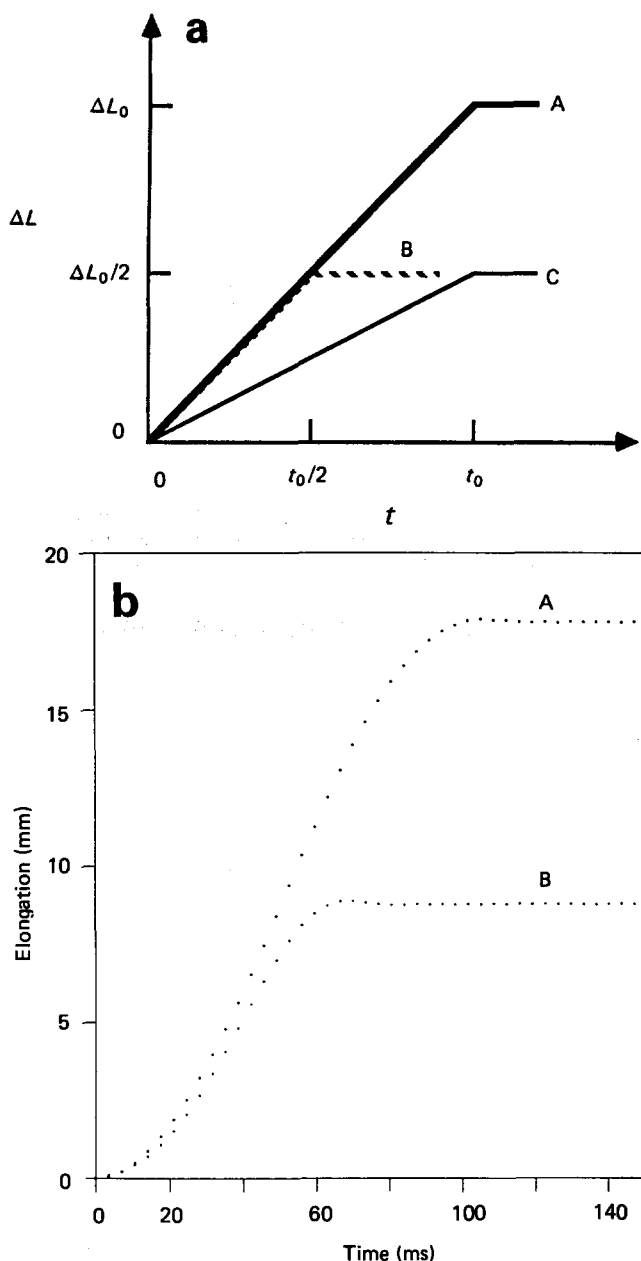


Figure 8 (a) Predicted elongation–time curves for (A) full fibre, (B) half-length one nucleus and (C) half-length polynucleation (b) Experimental curves for $\sigma = 98 \text{ kg cm}^{-2}$ and $T = 230^\circ\text{C}$: (A) full length fibre and (B) half-length fibre

from Figure 7 are 8, 2 and $1.9 \text{ kcal mol}^{-1}$ for $\sigma = 72, 98$ and 170 kg cm^{-2} , respectively. It is to be noted that $E_a = 8 \text{ kcal mol}^{-1}$ is in the range of activation energies commonly found for viscous flow for polymers above the glass transition temperature^{13,14}. The lower activation energy value (2 kcal mol^{-1}) likely manifests a strongly coupled (cooperative) phenomenon.

X-ray pinhole patterns of fibres heat treated at 140°C under a stress of 72 kg cm^{-2} , and 230°C and 170 kg cm^{-2} are shown in Figures 3b and 3c respectively.

DISCUSSION

The pinhole diffraction results show unambiguously that fibre elongation and crystallization are related; even at the lowest temperature and stress used, the product was semicrystalline. More conjectural is the interpretation of the observed three crystallization stages. However, the

contrast in the sharpness of the diffraction peaks between Figures 3b (lowest stress and temperature) and 3c (highest stress and temperature) may provide a clue. The fibre of Figure 3b underwent only the first stage of crystallization and exhibits relatively poorly developed diffraction peaks. The fibre of Figure 3c, on the other hand, experienced all stages of crystallization and exhibits well developed diffraction peaks. This suggests that imperfect crystals develop in stage I and that perfection increases in stage II and/or stage III. Stages I and II are differentiable only at the lowest stress used, and, at that stress, the time separation of the two stages decreases with increasing temperature. It is likely that these two stages (processes) merge under higher internal stress and that this is why no differentiation of these stages is found at the higher applied stress levels. Stage III is observed only as the specimens cool towards room temperature. Such crystallization under cool-down is typical in unoriented polymer systems^{15–18} and represents the crystallization of previously uncrystallized matter. If the same is true in the present case, then it is stage II that must represent a process (or processes) associated with increasing perfection of the crystallized regions. Such a sequence—initial formation of imperfect crystals, followed by reorganization—has been suggested previously^{5,9,12,21}. Considerable further work is needed in order to establish precisely the nature of the observed crystallization stages and their implications in terms of extant theories of crystallization under high molecular orientation^{19–21}.

In all previous investigations of the microstructure of material crystallized under high stress, it has been shown that the crystalline entities are thin fibrils, with the chain and fibril axes coincident. It is nearly certain that crystallization in the present case also has this fibrillar habit. Under this assumption, there are two questions which may be addressed:

(1) Are the fibrils long enough that nucleation need occur only once in the columnar locus of a fibril or, on the other hand, is there polynuclear crystallization along that columnar locus?

(2) What is the growth rate of a fibrillar crystal?

These questions are attacked in a simple experiment. If the length of the sample is reduced to one-half the original length, the elongational kinetics will be different for the mono- and polynuclear cases, in comparison to the elongation of the entire fibre. For the limiting case of mononuclear crystallization, the elongational rate of half- and full-length fibres (curves A and B of Figure 8a) should be identical. For dense polynuclear crystallization, the rate of elongation of the half-length fibre should be half of the original rate (curve C of Figure 8a). The result of such an experiment is presented in Figure 8b. Taking into account the non-linearity at the beginning of the process, one concludes that the crystallization is one-centre-like. Under this assumption, crystallization velocities are computed from Figures 5 and 6 and the length of the fibre (5 cm). Crystallization velocities of $75 \pm 5 \text{ cm s}^{-1}$ for the one- and two-stage transformations and $T \geq 200^\circ\text{C}$ is found. This value should be regarded as an upper estimate until confirmed by more detailed experiments.

SUMMARY

A 'splash heating' device to bring polymer fibres rapidly ($\sim 16 \text{ ms}$) to a temperature for heat treatment and to

maintain that temperature for some 300 ms is described. Initial measurements on PET fibres show a large dependence on stress and temperature. Under low stress, a multistage transformation occurs; at higher stresses, the first two stages merge. X-ray pinhole patterns suggest that the first two stages relate to (i) the development of imperfect crystals and (ii) a process whereby the perfection of the crystals increases. An experiment using fibres of different length suggests that long crystallites develop, each growing from a single nucleus.

ACKNOWLEDGEMENTS

The authors wish to thank Dr I. Avramov from the Bulgarian Academy of Sciences for helpful discussions. This work was supported by the National Science Foundation, under Grant CPE 830 4058.

REFERENCES

- 1 Smith, F. S. and Steward, R. D. *Polymer* 1974, **15**, 283
- 2 Alfonso, G. C., Verdoni, M. P. and Wasiak, A. *Polymer* 1978, **19**, 711
- 3 Althen, G. and Zachmann, H. G. *Makromol. Chem.* 1979, **180**, 2723
- 4 Kitao, T., Spruiell, J. E. and White, J. L. *Polym. Eng. Sci.* 1979, **19**, 761
- 5 Gupte, K. M., Motz, H. and Schultz, J. M. *J. Polym. Sci., Polym. Phys. Edn.* 1983, **21**, 1927
- 6 Elsner, G., Koch, M. H. J., Bordas, J. and Zachmann, H. G. *Makromol. Chem.* 1981, **182**, 1263
- 7 Peszkin, P. N. and Schultz, J. M. *J. Appl. Polym. Sci.* 1985, **30**, 2689
- 8 Desai, P. and Abhiraman, A. S. *J. Polym. Sci., Polym. Phys. Edn.* 1985, **23**, 653
- 9 Peszkin, P. N., Schultz, J. M. and Lin, J. S. *J. Polym. Sci., Polym. Phys. Edn.* 1986, **24**, 2591
- 10 Desai, P. and Abhiraman, A. S. *J. Polym. Sci., Polym. Lett. Edn.* 1986, **C24**, 135
- 11 Magill, J. H. and Schultz, J. M. 'Treatise on Materials Science', Vol. X, 'Properties of Solid Polymeric Materials', Academic Press, New York, 1977
- 12 Elad, J. and Schultz, J. M. *J. Polym. Sci., Polym. Phys. Edn.* 1984, **22**, 781
- 13 Rosen, S. L. 'Fundamental Principles of Polymeric Materials for Practising Engineers', Barnes and Noble, New York, 1971, p. 173
- 14 Beuche, F. 'Physical Properties of Polymers', Wiley-Interscience, New York, 1962, p. 91
- 15 Schultz, J. M., Robinson, W. H. and Ound, G. M. *J. Polym. Sci. (A-2)* 1967, **5**, 511
- 16 Schultz, J. M., Lin, J. S., Hendricks, R. W., Lagasse, R. R. and Kepler, R. G. *J. Appl. Phys.* 1980, **51**, 5508
- 17 Magill, J. H., Schultz, J. M. and Lin, J. S. *Colloid Polym. Sci.* 1987, **265**, 193
- 18 Schultz, J. M. *Makromol. Chem.* in press
- 19 Tiller, W. A. and Schultz, J. M. *J. Polym. Sci., Polym. Phys. Edn.* 1984, **22**, 143
- 20 Krigbaum, W. and Roe, R.-J. *J. Polym. Sci. (A)* 1964, **2**, 4391
- 21 Abhiraman, A. *J. Polym. Sci., Polym. Phys. Edn.* 1983, **21**, 583